

# Decisive Role of Perimeter Sites in Silica-Supported Ag Nanoparticles in Selective Hydrogenation of CO<sub>2</sub> to Methyl Formate in the Presence of Methanol

Juan José Corral-Pérez,<sup>†</sup> Atul Bansode,<sup>†</sup> C. S. Praveen,<sup>‡,§</sup> Anton Kokalj,<sup>||</sup> Helena Reymond,<sup>⊥</sup> Aleix Comas-Vives,<sup>§, #</sup> Joost VandeVondele,<sup>‡</sup> Christophe Copéret,<sup>§</sup> Philipp Rudolf von Rohr,<sup>⊥</sup> and Atsushi Urakawa<sup>\*, †</sup>

<sup>†</sup>Institute of Chemical Research of Catalonia (ICIQ), The Barcelona Institute of Science and Technology, 43007 Tarragona, Spain

<sup>‡</sup>Department of Materials, ETH Zürich, CH-8093 Zürich, Switzerland

<sup>§</sup>Department of Chemistry and Applied Biosciences, ETH Zürich, CH-8093 Zürich, Switzerland

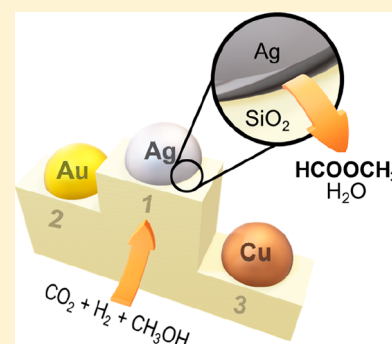
<sup>||</sup>Department of Physical and Organic Chemistry, Jožef Stefan Institute, SI-1000 Ljubljana, Slovenia

<sup>⊥</sup>Department of Mechanical and Process Engineering, ETH Zürich, CH-8092 Zürich, Switzerland

<sup>#</sup>Departament de Química, Universitat Autònoma de Barcelona, 08193 Cerdanyola del Vallès, Catalonia, Spain

## Supporting Information

**ABSTRACT:** Methyl formate synthesis by hydrogenation of carbon dioxide in the presence of methanol offers a promising path to valorize carbon dioxide. In this work, silica-supported silver nanoparticles are shown to be a significantly more active catalyst for the continuous methyl formate synthesis than the known gold and copper counterparts, and the origin of the unique reactivity of Ag is clarified. Transient in situ and operando vibrational spectroscopy and DFT calculations shed light on the reactive intermediates and reaction mechanisms: a key feature is the rapid formation of surface chemical species in equilibrium with adsorbed carbon dioxide. Such species is assigned to carbonic acid interacting with water/hydroxyls on silica and promoting the esterification of formic acid with adsorbed methanol at the perimeter sites of Ag on SiO<sub>2</sub> to yield methyl formate. This study highlights the importance of employing combined methodologies to verify the location and nature of active sites and to uncover fundamental catalytic reaction steps taking place at metal–support interfaces.



## INTRODUCTION

Methyl formate (MF) is a building block molecule in C<sub>1</sub> chemistry as well as a possible intermediate to produce chemical energy carriers.<sup>1</sup> This molecule can be used to produce several industrially important chemicals such as acetic acid,<sup>2</sup> ethylene glycol,<sup>3</sup> methanol, and formic acid.<sup>4</sup> In particular, both formic acid and methanol can be obtained simultaneously by simple hydrolysis reaction of MF. Commercially, MF is produced by the reaction of carbon monoxide (CO) and methanol<sup>5</sup> or via dehydrogenation of methanol.<sup>6</sup> Other synthesis routes like oxidative dehydrogenation of methanol<sup>7</sup> and dimerization of formaldehyde<sup>8</sup> have also been actively investigated. Among the alternative routes, the synthesis of MF from CO<sub>2</sub> and H<sub>2</sub> has recently attracted attention<sup>9,10</sup> owing to the increasing pressure to valorise CO<sub>2</sub> with the aim to mitigate its notorious impacts on climate change and to reduce our dependency on fossil fuels, provided that H<sub>2</sub> is produced from renewable and intermittent energy sources.<sup>11</sup>

A few approaches have been reported to produce MF from CO<sub>2</sub>, for instance, by photocatalytic reduction of CO<sub>2</sub><sup>12,13</sup> and CO<sub>2</sub> hydrogenation in the presence of methanol (eq 1). The

latter was demonstrated using both homogeneous<sup>14–16</sup> and heterogeneous catalysts.<sup>9,10,17,18</sup> Generally, heterogeneous catalysis offers great advantages to transform a large amount of reactant(s) with increased space-time-yield and benefits from process intensification associated with continuous operation, more facile product/catalyst separation, and catalyst regeneration. In fact, an efficient heterogeneous catalyst that promotes such a reaction would be key in developing the continuous synthesis of thermodynamically unstable formic acid starting from CO<sub>2</sub> and H<sub>2</sub>,<sup>19</sup> since MF can serve as an intermediate and methanol can also be produced by CO<sub>2</sub> hydrogenation.<sup>19</sup>



Only Cu and Au supported on metal oxides were reported as heterogeneous catalysts for the CO<sub>2</sub> hydrogenation to MF under batch rather than flow conditions.<sup>9,10,17,18</sup> Interestingly, Ag has not been investigated so far despite its similarity to Cu in terms of hydrogenation activity.<sup>20,21</sup> Other metals such as

Received: August 16, 2018

Published: September 30, 2018

Ru, Ni, and Pd were reported as promoters to Cu/ZnO/Al<sub>2</sub>O<sub>3</sub> catalyst positively influencing the yield of MF.<sup>17</sup> Among Au catalysts, the ZrO<sub>2</sub> supported ones show higher activities compared to those supported on CeO<sub>2</sub> and TiO<sub>2</sub>; this difference was ascribed to the amphoteric nature of the support, i.e., the acidic and basic sites promoting the adsorption of CO<sub>2</sub> and desorption of formic acid intermediate, respectively.<sup>9</sup> Support effects were also evidenced with Au/Al<sub>2</sub>O<sub>3</sub> which provides a 2-fold increase in yield by comparison to Au/TiO<sub>2</sub>.<sup>10</sup> These studies reveal the importance of appropriate combination of metal and support for improving the catalytic performance in the CO<sub>2</sub> hydrogenation to MF.

However, to date, the roles of metal and support as well as reaction mechanisms including the type of reactive surface species have not been clarified. It has been proposed that MF is formed by a reaction of CH<sub>3</sub>OH with either surface formates or formic acid intermediates.<sup>9,17,18</sup> This was supported by the lack of MF production in the absence of CH<sub>3</sub>OH<sup>17</sup> despite the formation of formate species on the catalyst surface as suggested by ex situ IR studies.<sup>10,18</sup> Therefore, it remains a challenge to determine the reactive intermediates and active sites that control the catalytic activity in the MF synthesis under reaction conditions.

In this work, we thus explore the reactivity of silica-supported Ag nanoparticles in comparison to the corresponding Cu and Au systems for continuous MF synthesis from CO<sub>2</sub> and H<sub>2</sub> in the presence of CH<sub>3</sub>OH. In situ and operando vibrational spectroscopic studies together with DFT calculations are performed to identify the reactive intermediate species and verify the location and nature of active sites and the underlying hypothesis of MF synthesis involving the reaction of surface formates.

## RESULTS AND DISCUSSION

**Catalytic Activity.** Catalysts based on Cu, Ag, and Au nanoparticles (<11 nm at 1 wt % metal loading; [Supporting Information](#), Table S4) supported on silica (155 m<sup>2</sup> g<sup>-1</sup>) are prepared by wetness impregnation method. Silica is chosen as a neutral support in order to probe the specific reactivity of the three different metals in the hydrogenation of CO<sub>2</sub> in the presence of methanol at 160 and 300 bar ([Figure 1](#)). At 300 bar, CH<sub>3</sub>OH conversion to MF increases significantly at higher temperatures in the order of the Ag > Au > Cu catalysts, while no activity is found for silica in the absence of metal particles (data not shown). For the Ag and Cu catalysts, the MF selectivity remains almost constant at around 100% at all temperatures examined, whereas the formation of carbon monoxide ( $S_{\text{CO}} = 19.7\%$ ) is observed at 280 °C and 300 bar with Au/SiO<sub>2</sub>. Although high MF selectivity (>99.9%) has been reported for Au/ZrO<sub>2</sub> catalyst at lower temperature and pressure (200 °C and 160 bar) under batch operation,<sup>9</sup> gold nanoparticles supported on different metal oxides are known to be catalytically active for the water–gas shift reaction and its reverse reaction, i.e., CO<sub>2</sub> hydrogenation to produce CO, favored at higher temperatures.<sup>22</sup> It is worth highlighting that increasing the reaction pressure from 160 to 300 bar results in a drastic increase in the MF yield. Assuming that MF is formed via the reaction of CH<sub>3</sub>OH and surface formates, this result suggests that the formation of reactive formate species is promoted at higher pressure in addition to the kinetic advantages induced by the higher fluid density and the enhanced actual contact time of the reactants with the

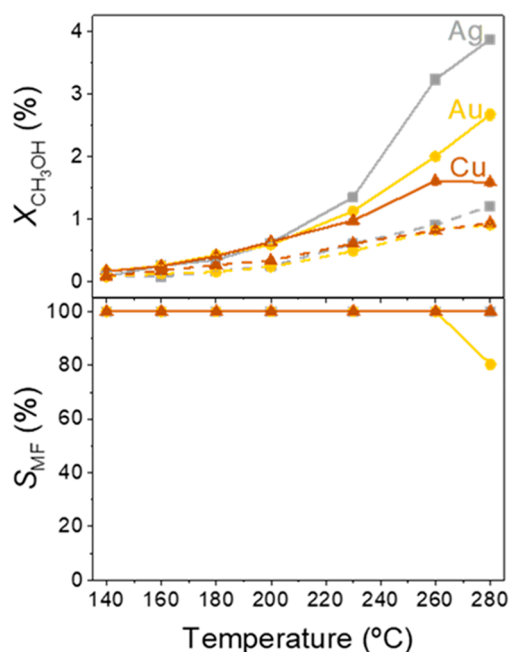


**Figure 1.** Effects of temperature and pressure on CH<sub>3</sub>OH conversion ( $X_{\text{CH}_3\text{OH}}$ ) and selectivity to MF ( $S_{\text{MF}}$ ) over silica-supported 1 wt % metal catalysts. Reaction conditions: CO<sub>2</sub>:H<sub>2</sub>:CH<sub>3</sub>OH = 4:4:1 (molar ratio), pressure = 160 bar (dashed line) and 300 bar (solid line), GHSV = 9000 h<sup>-1</sup>.

catalysts, as previously observed for CH<sub>3</sub>OH synthesis via CO<sub>2</sub> hydrogenation.<sup>23,24</sup>

**Surface Species Involved in CO<sub>2</sub> Hydrogenation.** In situ DRIFTS and Raman measurements are performed to gain insights into the surface species formed from CO<sub>2</sub> and H<sub>2</sub> that may be linked to MF formation. As depicted in [Figure 2](#), similar surface formate species with characteristic bands at 1600, 1688, 2711, 2817, and 2952 cm<sup>-1</sup> are observed for the three catalysts under the mixture of CO<sub>2</sub> and H<sub>2</sub> (1:1 molar ratio) at 230 °C. In Raman spectra ([Figure 2](#)), the bands at 1330 and 1580 cm<sup>-1</sup>, also assigned to surface formates,<sup>25</sup> appear after exposing Cu/SiO<sub>2</sub> catalyst to reactant mixture at 200 and 400 bar.

Increasing the pressure of CO<sub>2</sub> and H<sub>2</sub> in the DRIFTS and Raman cells up to their respective maximum technical limits results in a drastic increase in the concentration of formate species as confirmed by the increased absorbance of their bands ([Figure 2](#)). This is also consistent with the higher MF yield observed at higher pressure ([Figure 1](#)). Although spectral features are similar for Cu, Ag, and Au as expected from DFT calculations ([Supporting Information](#), Table S5), more pronounced formation of formate species over Ag/SiO<sub>2</sub> compared to Cu/SiO<sub>2</sub> and Au/SiO<sub>2</sub> is evident at higher pressure ([Supporting Information](#), Table S7). This trend is also consistent with more facile formation of stable  $\kappa^2$ -formate (typically called bidentate formate) over the Ag surface as predicted by DFT calculations, i.e., calculated activation barriers for formate formation are 0.61, 0.71, and 0.97 eV on Ag, Cu, and Au, respectively ([Supporting Information](#), section S1.1). Based on the DFT results, we find that the activation energy for the formation of surface formates (HCOO) is simply given by the interplay between weak and strong adsorption bonding of H and HCOO, respectively. The relation between the activation energies ( $E^*$ ) and the

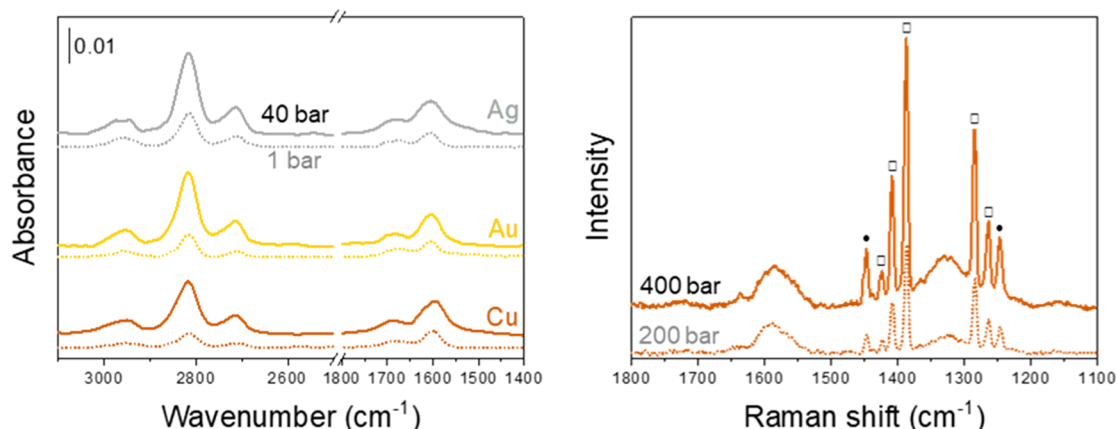


**Figure 2.** In situ DRIFT and Raman spectra of supported 1 wt % metal catalysts upon exposure to  $\text{CO}_2:\text{H}_2 = 1:1$  (molar ratio) at 230 °C. (Left) In situ DRIFT spectra at pressure = 1 (dashed line) and 40 (solid line) bar. (Right) In situ Raman spectra of 1 wt % Cu/SiO<sub>2</sub> at pressure = 200 (dashed line) and 400 (solid line) bar. Characteristic bands due to the reactant mixture are shown with symbols: CO<sub>2</sub> (●) and H<sub>2</sub> (□).

adsorption binding energies of  $\kappa^2\text{-HCOO}$  ( $E_b^{\text{HCOO}}$ ) and H ( $E_b^{\text{H}}$ ) is shown in Figure 3, while the corresponding activation

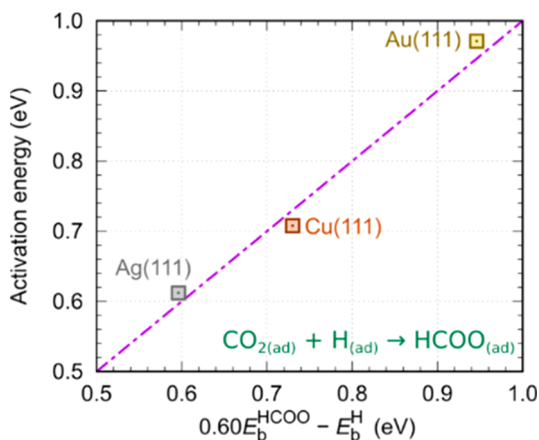


**Figure 3.** Correlation between the PBE-D<sup>2</sup>/plane-wave calculated<sup>29</sup> and estimated activation energies for the formate formation on Cu(111), Ag(111), and Au(111); PBE-D<sup>2</sup> stands for PBE functional<sup>30</sup> with reparametrized D2 dispersion correction of Grimme.<sup>31</sup> The activation energy estimator,  $E^* \approx 0.6E_b^{\text{HCOO}} - E_b^{\text{H}}$ , is derived in the Supporting Information, section S1.1.1.  $E_b^{\text{HCOO}}$  and  $E_b^{\text{H}}$  are the adsorption binding energies of bidentate  $\kappa^2\text{-HCOO}$  and H, respectively. The RMS error of the estimator is 0.03 eV and the largest error is 0.03 eV.

energy estimator,  $E^* \approx 0.6E_b^{\text{HCOO}} - E_b^{\text{H}}$ , is derived in Supporting Information, section S1.1.1. The lowest energy barrier for formate formation over Ag can be thus attributed to its weak binding to H and sufficiently strong binding to HCOO. Both factors promote this reaction step in a synergistic way, since one reactant is destabilized (H) while the product is stabilized (HCOO). In contrast, Au binds HCOO too weakly, whereas Cu binds H too strongly.

As indicated by catalytic and in situ spectroscopic results, the concentration of surface formate species is directly linked to the MF yield. To gain more information about the nature of the observed surface species (Figure 2), a transient in situ DRIFTS study is performed by passing alternatively the reactant gas ( $\text{CO}_2:\text{H}_2$  at 1:1 molar ratio) and an inert gas (Ar) over 1 wt % Ag/SiO<sub>2</sub> catalyst at 230 °C (Figure 4a). Under these conditions, the bands at 2711, 2817, and 2952 cm<sup>-1</sup> in

the  $\nu(\text{C-H})$  region gradually appear and disappear, apparently in a synchronized fashion with the band at 1600 cm<sup>-1</sup>, confirming their attribution to  $\kappa^2\text{-formate}$  species over the Ag surface.<sup>26–28</sup> This assignment is consistent with DFT calculations (Supporting Information, Table S5) and their identical temporal evolutions of kinetically distinguishable component spectra (i.e., spectra with chemically distinct origins) extracted by a multivariate spectral analysis (Figure 4b,c,  $\kappa^2\text{-HCOO}$ ).

On the other hand, the chemical origin of the band at 1688 cm<sup>-1</sup> is more difficult to elucidate. However, the possible candidate species are formates, carbonates, formic acid, and carbonic acid ( $\text{H}_2\text{CO}_3$ ). DFT calculations reveal that monodentate  $\kappa^1\text{-formate}$  species are too short-lived to be observed by vibrational spectroscopy (Supporting Information, Table S6) although they display  $\nu(\text{C-O})$  frequency in the same range (Supporting Information, Table S5). Neither can they be carbonates since their  $\nu(\text{C-O})$  frequency changes significantly depending on the studied metal (Supporting Information, Table S5). According to DFT calculations, formic acid would be a good candidate, displaying the matching  $\nu(\text{C-O})$  frequency (Supporting Information, Table S5). However, from the experimental counterpart, the absence of the characteristic band in the  $\nu(\text{C-H})$  region with the identical temporal profile as that at 1688 cm<sup>-1</sup> speaks against its attribution to formic acid or related species. This makes carbonic acid a sound potential candidate. According to DFT calculations it displays a matching  $\nu(\text{C-O})$  frequency (Supporting Information, Table S5), and furthermore, it lacks the C-H bonds thus supporting the absence of the characteristic band in the  $\nu(\text{C-H})$  region.

To corroborate the assignment of the 1688 cm<sup>-1</sup> band, we performed further analysis. A deeper look into the spectral region where a strong signal of gaseous CO<sub>2</sub> dominates (Supporting Information, Figure S9a) shows the presence of a band at 2341 cm<sup>-1</sup>, which overlaps with the bands of gaseous CO<sub>2</sub> but is kinetically separable (Supporting Information, Figure S9b). This identification is possible thanks to the disentangling power of the multivariate spectral analysis and the plug-flow design of the DRIFTS cell with minimized gas volume,<sup>32</sup> thereby enhancing signals from surface species. Importantly, the comparison of the concentration profiles of the kinetically pure component spectra clarifies that the band at 1688 cm<sup>-1</sup> behaves kinetically identical to the band at 2341



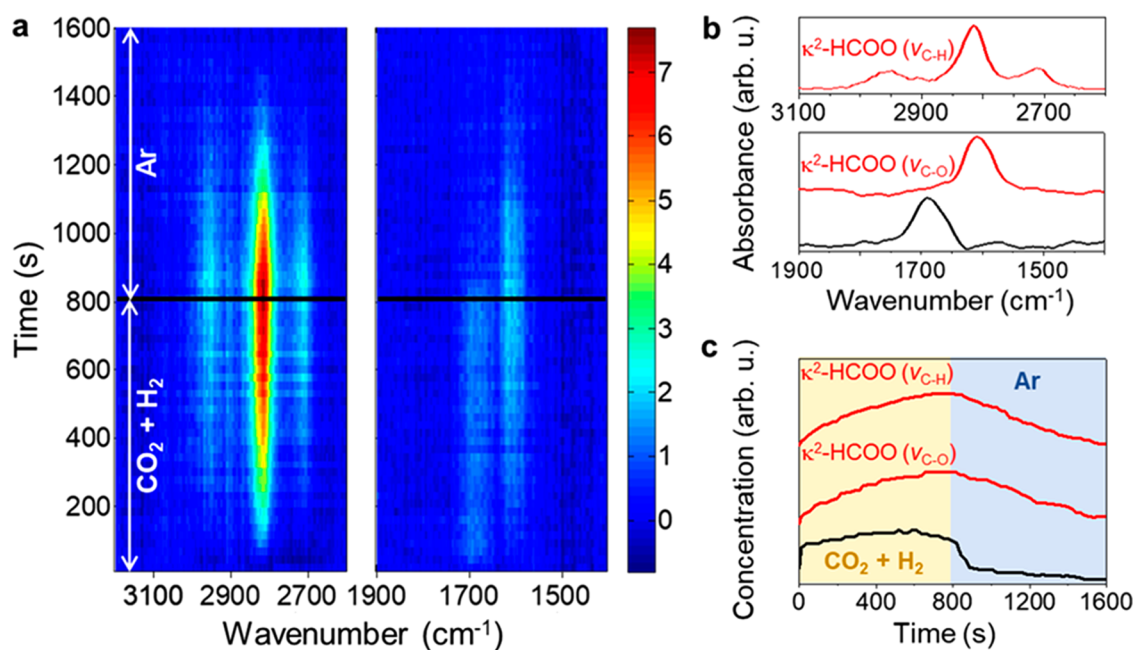


**Figure 4.** Transient DRIFTS study on CO<sub>2</sub> hydrogenation over 1 wt % Ag/SiO<sub>2</sub> catalyst. (a) Time-resolved DRIFT spectra upon exposure to CO<sub>2</sub>:H<sub>2</sub> = 1:1 molar ratio (the first half period) and then to Ar (the second half period) concentration perturbation experiment at 230 °C and 5 bar. The DRIFT spectra are shown in milli-absorbance unit taking the last spectrum in the Ar atmosphere as background. (b) Components spectra obtained by multivariate spectral analysis applied on the time-resolved DRIFT spectra. (c) Concentration profiles of the corresponding components spectra obtained by the multivariate spectral analysis.

cm<sup>-1</sup> for both SiO<sub>2</sub> and Ag/SiO<sub>2</sub> (Figure 4c, Supporting Information, Figures S9 and S10). This observation suggests that the two bands at 1688 and 2341 cm<sup>-1</sup> originate either from the same surface chemical species or from kinetically indistinguishable species appearing at the same time. Isotopic labeling studies using <sup>13</sup>CO<sub>2</sub> and D<sub>2</sub> (Supporting Information, Figure S13) show that both bands are due to the vibration of C–O bonds, with a negligible involvement of hydrogen for the band at 1688 cm<sup>-1</sup>.

In the literature, the band at 2341 cm<sup>-1</sup> has been reported and assigned to asymmetric stretching of CO<sub>2</sub> adsorbed on SiO<sub>2</sub> due to its interaction with silanol groups.<sup>33–35</sup> Also, a transient in situ DRIFTS study performed by alternately passing CO<sub>2</sub> (without H<sub>2</sub>) vs Ar over bare SiO<sub>2</sub> reveals the emergence of the same band at 2341 cm<sup>-1</sup> under CO<sub>2</sub> (Supporting Information, Figure S10). The involvement of the OH groups on SiO<sub>2</sub> during the CO<sub>2</sub> sorption process is also evident from the apparent, reversible decrease of the OH bands upon CO<sub>2</sub> admission (Supporting Information, Figure S11). The different chemical nature of the two kinetically indistinguishable bands is indeed confirmed by their intensity ratio ( $I_{2341}/I_{1688}$ ), which varies under different reaction conditions (CO<sub>2</sub> vs Ar and CO<sub>2</sub> + H<sub>2</sub> vs Ar) over Ag/SiO<sub>2</sub> and SiO<sub>2</sub>, respectively (Supporting Information, Table S8). It is worth noting that the intensity of the band at 1688 cm<sup>-1</sup> is higher (smaller value of the  $I_{2341}/I_{1688}$  ratio) in the presence of H<sub>2</sub>, indicating direct/indirect involvement of hydrogen in the formation or stabilization of the surface chemical species corresponding to this band.

The spectral characteristics indicated that the surface species is possibly carbonic acid. Thus, we evaluated by DFT calculations the formation of carbonic acid on a surface model of highly hydroxylated SiO<sub>2</sub> (Figure 5a)<sup>36</sup> and found that this species is significantly stabilized by the formation of multiple hydrogen-bonds present on the SiO<sub>2</sub> surface (Figure

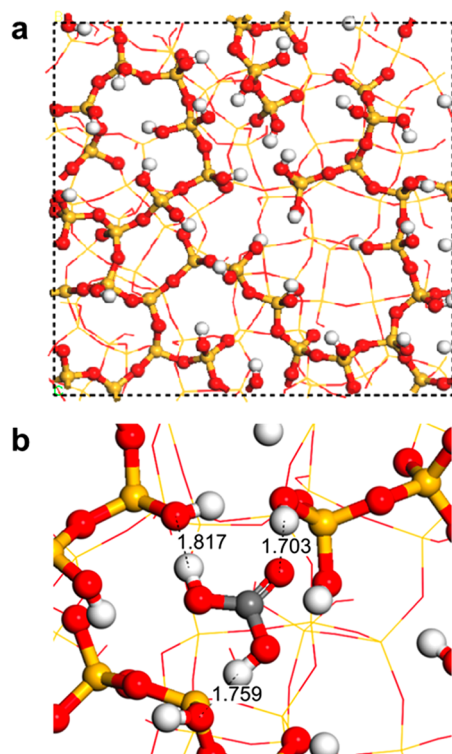


**Figure 5.** (a) Top view of the optimized structure of the hydroxylated SiO<sub>2</sub> surface (7.2 OH nm<sup>-2</sup>). (b) The most stable identified structure of carbonic acid adsorbed on the SiO<sub>2</sub> surface as obtained from PBE-D3/DZVP calculations. The representative distances, which characterize the hydrogen-bonds of carbonic acid with silanols of the SiO<sub>2</sub> surface are shown in Å.

Sb). The most favorable structures of adsorbed carbonic acid are those formed through the reaction of CO<sub>2</sub> with adsorbed

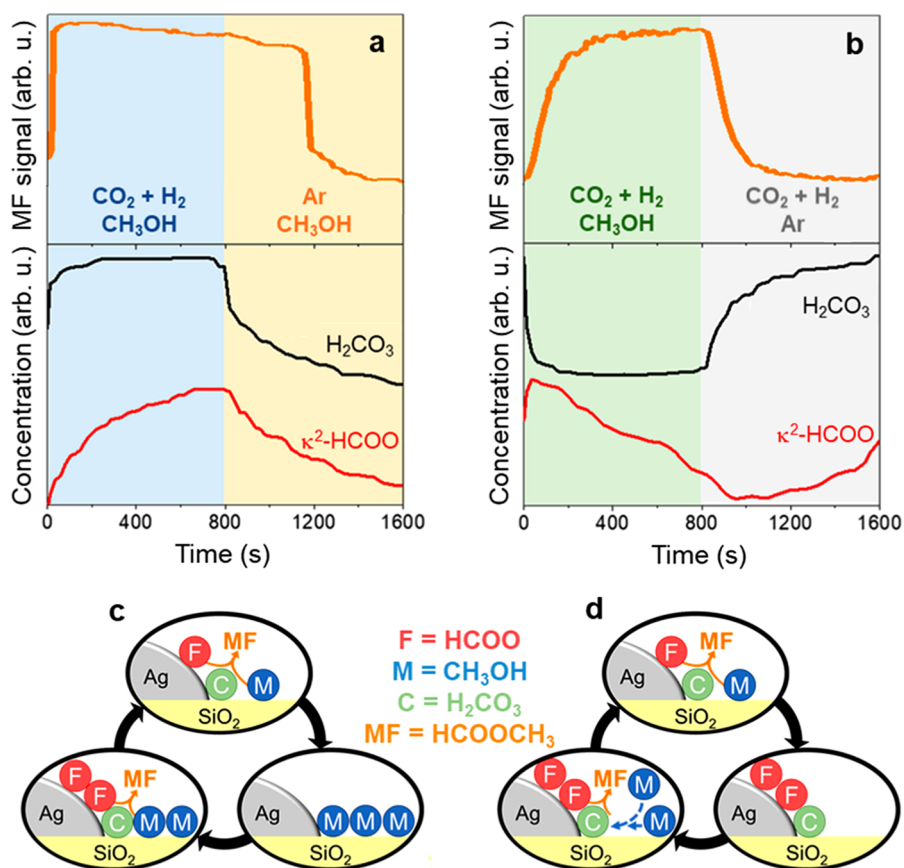


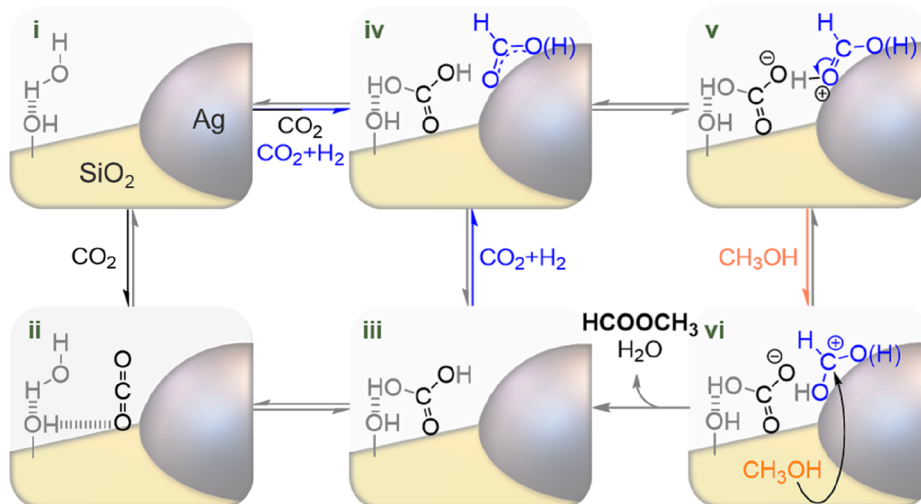
**Figure 6.** Operando DRIFTS studies on the esterification of formates with CH<sub>3</sub>OH to MF over 1 wt % Ag/SiO<sub>2</sub>. (a and b) MS signal of MF ( $m/z = 60$ , top graphs) and concentration profiles of adsorbed carbonic acid and  $\kappa^2$ -formates obtained by the multivariate spectral analysis (bottom graphs). The analysis was applied on the time-resolved DRIFT spectra of 1 wt % Ag/SiO<sub>2</sub> upon exposure to (a) CO<sub>2</sub> + H<sub>2</sub> + CH<sub>3</sub>OH (the first half) vs Ar + CH<sub>3</sub>OH (the second half period), and (b) CO<sub>2</sub> + H<sub>2</sub> + CH<sub>3</sub>OH (the first half) vs CO<sub>2</sub> + H<sub>2</sub> + Ar (the second half period) at 230 °C and 5 bar (total pressure). (c and d) Suggested mechanisms for the formation of MF from CO<sub>2</sub>, H<sub>2</sub>, and CH<sub>3</sub>OH in studies a and b, respectively.

water rather than with a gaseous water molecule. The reaction Gibbs energy for this structure (Figure 5b) is slightly endergonic at 230 °C and 5 bar (+0.49 eV), which may explain the necessity for higher pressure to boost its formation and consequently the catalytic activity, provided that this species is involved in the reaction mechanism. Alternatively, defects on the SiO<sub>2</sub> surface, which are not taken into account in our surface model, may further stabilize its formation. Hence, all data above and DFT calculations (Supporting Information, section S1.3) point to the attribution of the band at 1688 cm<sup>-1</sup> to carbonic acid adsorbed on highly hydroxylated silica in equilibrium with adsorbed CO<sub>2</sub> and H<sub>2</sub>O; note that H<sub>2</sub>O is assumed to be present on the silica surface due to its pretreatment.<sup>36</sup> Such species is likely formed in a microporous/defect region of the silica support or at the interface between silica and Ag nanoparticles where such adsorption would be favored.

Curiously, the amount of adsorbed CO<sub>2</sub>, indicated by the band at 2341 cm<sup>-1</sup>, is boosted when Ag is present on the SiO<sub>2</sub> surface (Supporting Information, Figure S12), probably because Ag-SiO<sub>2</sub> interaction enhances the number of adsorption sites (i.e., hydroxyl groups) at the perimeter of Ag particles on SiO<sub>2</sub>.<sup>24</sup> Consequently, a facilitated formation of adsorbed carbonic acid at/near the perimeter sites can be assumed. This implied importance of the perimeter sites is in line with the smaller pressure-dependency of the amount of adsorbed carbonic acid observed at 1688 cm<sup>-1</sup> compared to

that of  $\kappa^2$ -formate on Ag observed at 1600 cm<sup>-1</sup> (Figure 2, Supporting Information, Table S7). The restricted number of the active sites at the perimeter and their expectedly higher reactivity explain the relatively constant concentration of the former against pressure variations, while the high pressure-dependency of the latter (Figure 2) indicates varying coverage of surface formates on Ag dynamically responding to the reactant pressure.

**Mechanistic Insights into MF Formation.** According to the above observations, Ag enhances CO<sub>2</sub> adsorption and carbonic acid formation, possibly rendering the Ag-SiO<sub>2</sub> interface more active for specific catalytic transformations. To better understand the role of active surface species and where the reaction takes place, transient DRIFTS measurements under operando conditions (i.e., simultaneous reactivity measurements by mass spectrometry (MS)) are performed. Despite the lower pressure (5 bar) of these experiments due to technical limitations, the reactivity could be evaluated to firmly establish relationships among catalyst structure, surface intermediates and catalytic activity. In the first experiment, Ag/SiO<sub>2</sub> is first pre-exposed to the gas flow of CO<sub>2</sub> + H<sub>2</sub> + CH<sub>3</sub>OH (vapor), followed by exposure to CH<sub>3</sub>OH and then switched back to CO<sub>2</sub> + H<sub>2</sub> + CH<sub>3</sub>OH. The two gas atmospheres are switched repeatedly and periodically. Similar to the identification of surface chemical species (Figure 4), the IR spectra of “kinetically separable” species and their concentration profiles are obtained by the multivariate spectral

Scheme 1. Proposed Mechanism for the CO<sub>2</sub> Hydrogenation to MF in the Presence of CH<sub>3</sub>OH over Ag/SiO<sub>2</sub><sup>a</sup>

<sup>a</sup>For further description, in particular the meaning of symbol "(H)", see text.

analysis of the time-resolved DRIFT spectra, firmly identifying the presence of adsorbed CH<sub>3</sub>OH (or methoxy), adsorbed CO<sub>2</sub>,  $\kappa^2$ -formates and adsorbed carbonic acid (Figure 6a and Supporting Information, Figure S15–S17). No spectral changes are observed when pure silica is used (Supporting Information, Figure S18), hence the spectral changes observed for Ag/SiO<sub>2</sub> stem from Ag or the Ag-SiO<sub>2</sub> interface.

When the atmosphere is changed from CH<sub>3</sub>OH to CO<sub>2</sub> + H<sub>2</sub> + CH<sub>3</sub>OH (the first half period of Figure 6a), a first rapidly increasing and then relatively constant MF production is observed. The MF formation profile upon the gas switching matches well with that of carbonic acid (Figure 6a) but inversely with that of adsorbed CH<sub>3</sub>OH (Supporting Information, Figure S17). Interestingly, when the reaction mixture is switched to CH<sub>3</sub>OH (the second half period), a lasting production of MF is observed until the surface concentrations of  $\kappa^2$ -formate and adsorbed carbonic acid are very low (Figure 6a). To gain further insights into the mechanism, a second operando DRIFTS study is performed by exposing the catalyst to the gas flow of CO<sub>2</sub> + H<sub>2</sub> and followed by alternately passing the flows of CO<sub>2</sub> + H<sub>2</sub> + CH<sub>3</sub>OH and CO<sub>2</sub> + H<sub>2</sub> (Figure 6b and Supporting Information, Figure S22–S24). In this case, the rapid and lasting formation of MF detected previously (Figure 6a) is not observed, and the amount of formed MF changes gradually in response to the switch of the gas atmosphere, specifically to methanol.

Importantly, the MF formation rate is not determined by the concentration of formates on Ag because the concentration profiles of surface formates and gaseous MF are uncorrelated (Figure 6a and 4b). The continuing formation of MF after switching from CO<sub>2</sub> + H<sub>2</sub> + CH<sub>3</sub>OH to CH<sub>3</sub>OH and the sudden ceasing of MF formation only after surface formates on Ag are mostly depleted (Figure 6a) imply that formates over the Ag surface gradually migrate toward the perimeter sites (spillover) for their further transformation to MF or formates formed at the interface remain there unless methanol reacts, even in the absence of CO<sub>2</sub> and H<sub>2</sub> in the atmosphere. Moreover, we assume that formates first transform into formic acid which then reacts with methanol to yield MF. In the presence of CO<sub>2</sub> and H<sub>2</sub>,  $\kappa^2$ -formates formed on Ag via CO<sub>2</sub> hydrogenation are expected to react with the surface H located

on Ag to yield formic acid. DFT calculations indeed support this scenario and show that Ag and Au are superior to Cu for formation of formic acid, i.e., the reaction is exothermic on Ag and Au and the activation barrier is low enough for reaction to be facile at 230 °C (Supporting Information, section S1.2). This is consistent with the catalytic results (Figure 1) and literature reports.<sup>9,10</sup> However, this path cannot explain the formation of MF in the absence of CO<sub>2</sub> and H<sub>2</sub> (Figure 6a). One plausible path is the proton transfer from the carbonic acid to surface formates at the perimeter sites where these surface species are known to be concentrated (vide supra). Thus, the spillover of formates on Ag allows retaining a constant amount of reactive formic acid formation at the perimeter sites so that such species react with methanol to yield MF (eq 2).



Furthermore, the availability of CH<sub>3</sub>OH that can react with formic acid also plays another critical role in the MF formation. CH<sub>3</sub>OH can strongly adsorb over SiO<sub>2</sub> (Supporting Information, Figure S19 and S20) and thus its availability near the active perimeter sites can lead to immediate formation of MF (Figure 6a) if CH<sub>3</sub>OH is continuously fed (Figure 6c). On the other hand, when it is discontinuously fed, MF concentration profile follows the expected profile of CH<sub>3</sub>OH vapor in the operando cell, manifesting that the adsorption and diffusion of CH<sub>3</sub>OH on the catalyst surface are rate-limiting due to the strong binding of CH<sub>3</sub>OH on SiO<sub>2</sub> under the evaluated transient conditions. The adsorbed CH<sub>3</sub>OH can be therefore depleted in the vicinity of Ag through MF formation (Figure 6d), which is why the adsorption of CH<sub>3</sub>OH and its access to the perimeter sites affect critically the MF formation rate.

On the basis of the in situ and operando studies described above, a mechanism for the CO<sub>2</sub> hydrogenation to MF in the presence of CH<sub>3</sub>OH over Ag/SiO<sub>2</sub> is proposed (Scheme 1i–vi). CO<sub>2</sub> is adsorbed on SiO<sub>2</sub> due to its interaction with silanol groups (i–ii). Carbonic acid in equilibrium with CO<sub>2</sub> and water adsorbed on SiO<sub>2</sub> near Ag is readily formed (iii, vide supra).  $\kappa^2$ -Formates (iv, without H in bracket) are formed from CO<sub>2</sub> and H<sub>2</sub> over the Ag surface and transformed to formic



acid either via hydrogenation with surface H (iv, with H in bracket) or via protonation through carbonic acid residing at the perimeter sites (v, without H in bracket). These formate or formic acid (v), that can also be protonated through carbonic acid, is the intermediate yielding MF through its reaction with surface adsorbed CH<sub>3</sub>OH (vi) as indicated by the abrupt decrease in the adsorbed CH<sub>3</sub>OH concentration (Supporting Information, Figure S17). The close match in the concentration profiles of carbonic acid and MF (Figure 6a and 4b) suggests that the esterification reaction between formic acid and methanol is accelerated by the presence of carbonic acid formed near the perimeter sites either through catalyzing formic acid formation or mediating the esterification reaction (Scheme 1). All of the results above converge to highlight the importance of the metal–support interface, particularly the perimeter sites, for the catalytic reaction. Also for a related reaction, hydrogenation of CO<sub>2</sub> to methanol, the transformation of the key formate intermediates to CH<sub>3</sub>OH<sup>19,23,24,37,38</sup> was reported to be favored at the metal–support interface for a Cu/ZrO<sub>2</sub> catalyst<sup>24,39</sup> and the current study further affirms the important roles of such sites. These mechanistic insights are highly important for the catalyst design since adsorption strength and diffusion rate of CH<sub>3</sub>OH, which affect the reaction rate, would be uniquely determined by the nature of support.

## CONCLUSION

In summary, we uncovered that Ag is particularly active among coinage metals in continuous MF synthesis from CO<sub>2</sub>, H<sub>2</sub> and CH<sub>3</sub>OH due to its superior activity in the formation of surface formates and subsequent formic acid. Ag displays the lowest activation barrier for the formation of formates, because it binds atomic hydrogen weakly and formates strong enough, whereas Au binds formates too weakly and Cu binds H too strongly. The nature of the surface species formed over the catalyst was unambiguously elucidated by transient in situ DRIFTS studies and DFT calculations. The use of transient operando vibrational spectroscopy identified Ag–SiO<sub>2</sub> interface as the active site in the formation of MF via the esterification of surface adsorbed methanol with formic acid in the presence of carbonic acid. Such a reaction is proposed to be promoted by carbonic acid in equilibrium with adsorbed CO<sub>2</sub> in interaction with water/hydroxyls on SiO<sub>2</sub>, a so-called neutral support. These insights and employed combined methodologies are expected to facilitate rational catalyst design by tuning active metal and support materials for this and other reactions.

## ASSOCIATED CONTENT

### Supporting Information

The Supporting Information is available free of charge on the ACS Publications website at DOI: 10.1021/jacs.8b08505.

DFT analysis, additional data, and experimental details (PDF)

## AUTHOR INFORMATION

### Corresponding Author

\*aurakawa@iciq.es

### ORCID

Anton Kokalj: 0000-0001-7237-0041

Helena Reymond: 0000-0001-5183-2446

Aleix Comas-Vives: 0000-0002-7002-1582

Joost VandeVondele: 0000-0002-0902-5111

Christophe Copéret: 0000-0001-9660-3890

Atsushi Urakawa: 0000-0001-7778-4008

## Notes

The authors declare no competing financial interest.

## ACKNOWLEDGMENTS

This work was conducted in the framework of the SNF Sinergia project (CRSII2-154448). J.J.C., A.B., and A.U. acknowledge Generalitat de Catalunya for financial support through the CERCA Programme and MINECO, Spain for financial support (CTQ2016-75499-R (FEDER-UE)) and for support through Severo Ochoa Excellence Accreditation 2014–2018 (SEV-2013-0319). A.K. acknowledges the financial support from the Slovenian Research Agency (Grant No. P2-0393). A.C.V. thanks the Holcim Foundation and Spanish MEC for a Ramon y Cajal research contract (RYC-2016-19930) and the European Social Fund. C.C. acknowledges the SCCER Heat and Energy Storage for financial support. Calculations were in part enabled by a grant from the Swiss National Supercomputer Center (CSCS) under project ID ch5.

## REFERENCES

- (1) Lee, J. S.; Kim, J. C.; Kim, Y. G. Methyl formate as a new building block in C<sub>1</sub> chemistry. *Appl. Catal.* **1990**, *57* (1), 1–30.
- (2) Jenner, G.; Nahmed, E. M. The cobalt-catalyzed conversion of methyl formate into acetic acid. *J. Organomet. Chem.* **1991**, *407* (1), 135–142.
- (3) Celik, F. E.; Lawrence, H.; Bell, A. T. Synthesis of precursors to ethylene glycol from formaldehyde and methyl formate catalyzed by heteropoly acids. *J. Mol. Catal. A: Chem.* **2008**, *288* (1–2), 87–96.
- (4) Reymond, H.; Vitas, S.; Vernuccio, S.; von Rohr, P. R. Reaction process of resin-catalyzed methyl formate hydrolysis in biphasic continuous flow. *Ind. Eng. Chem. Res.* **2017**, *56* (6), 1439–1449.
- (5) Di Girolamo, M.; Lami, M.; Marchionna, M.; Sanfilippo, D.; Andreoni, M.; Galletti, A. M. R.; Sbrana, G. Methanol carbonylation to methyl formate catalyzed by strongly basic resins. *Catal. Lett.* **1996**, *38* (1), 127–131.
- (6) Tonner, S. P.; Trimm, D. L.; Wainwright, M. S.; Cant, N. W. Dehydrogenation of methanol to methyl formate over copper catalysts. *Ind. Eng. Chem. Prod. Res. Dev.* **1984**, *23* (3), 384–388.
- (7) Kaichev, V. V.; Popova, G. Y.; Chesalov, Y. A.; Saraev, A. A.; Zemlyanov, D. Y.; Beloshapkin, S. A.; Knop-Gericke, A.; Schlögl, R.; Andrushkevich, T. V.; Bukhtiyarov, V. I. Selective oxidation of methanol to form dimethoxymethane and methyl formate over a monolayer V<sub>2</sub>O<sub>5</sub>/TiO<sub>2</sub> catalyst. *J. Catal.* **2014**, *311*, 59–70.
- (8) Mueller, L. L.; Griffin, G. L. Formaldehyde conversion to methanol and methyl formate on copper/zinc oxide catalysts. *J. Catal.* **1987**, *105* (2), 352–358.
- (9) Wu, C. Y.; Zhang, Z. F.; Zhu, Q. G.; Han, H. L.; Yang, Y. Y.; Han, B. X. Highly efficient hydrogenation of carbon dioxide to methyl formate over supported gold catalysts. *Green Chem.* **2015**, *17* (3), 1467–1472.
- (10) Filonenko, G. A.; Vrijburg, W. L.; Hensen, E. J. M.; Pidko, E. A. On the activity of supported Au catalysts in the liquid phase hydrogenation of CO<sub>2</sub> to formates. *J. Catal.* **2016**, *343*, 97–105.
- (11) Mikkelsen, M.; Jorgensen, M.; Krebs, F. C. The teraton challenge. A review of fixation and transformation of carbon dioxide. *Energy Environ. Sci.* **2010**, *3* (1), 43–81.
- (12) Chen, J. S.; Xin, F.; Qin, S. Y.; Yin, X. H. Photocatalytically reducing CO<sub>2</sub> to methyl formate in methanol over ZnS and Ni-doped ZnS photocatalysts. *Chem. Eng. J.* **2013**, *230*, 506–512.
- (13) Qin, S. Y.; Xin, F.; Liu, Y. D.; Yin, X. H.; Ma, W. Photocatalytic reduction of CO<sub>2</sub> in methanol to methyl formate over CuO–TiO<sub>2</sub> composite catalysts. *J. Colloid Interface Sci.* **2011**, *356* (1), 257–261.

- (14) Jessop, P. G.; Hsiao, Y.; Ikariya, T.; Noyori, R. Methyl formate synthesis by hydrogenation of supercritical carbon-dioxide in the presence of methanol. *J. Chem. Soc., Chem. Commun.* **1995**, No. 6, 707–708.
- (15) Krocher, O.; Koppel, R. A.; Baiker, A. Highly active ruthenium complexes with bidentate phosphine ligands for the solvent-free catalytic synthesis of N,N-dimethylformamide and methyl formate. *Chem. Commun.* **1997**, No. 5, 453–454.
- (16) Yadav, M.; Linehan, J. C.; Karkamkar, A. J.; van der Eide, E.; Heldebrant, D. J. Homogeneous hydrogenation of CO<sub>2</sub> to methyl formate utilizing switchable ionic liquids. *Inorg. Chem.* **2014**, 53 (18), 9849–9854.
- (17) Yu, K. M. K.; Yeung, C. M. Y.; Tsang, S. C. Carbon dioxide fixation into chemicals (methyl formate) at high yields by surface coupling over a Pd/Cu/ZnO nanocatalyst. *J. Am. Chem. Soc.* **2007**, 129 (20), 6360–6361.
- (18) Kerry Yu, K. M.; Tsang, S. C. A study of methyl formate production from carbon dioxide hydrogenation in methanol over a copper zinc oxide catalyst. *Catal. Lett.* **2011**, 141 (2), 259–265.
- (19) Álvarez, A.; Bansode, A.; Urakawa, A.; Bavykina, A. V.; Wezendonk, T. A.; Makkee, M.; Gascon, J.; Kapteijn, F. Challenges in the Greener Production of Formates/Formic Acid, Methanol, and DME by Heterogeneously Catalyzed CO<sub>2</sub> Hydrogenation Processes. *Chem. Rev.* **2017**, 117 (14), 9804–9838.
- (20) Oakton, E.; Vile, G.; Levine, D.; Zocher, E.; Baudouin, D.; Perez-Ramirez, J.; Coperet, C. Silver nanoparticles supported on passivated silica: preparation and catalytic performance in alkyne semi-hydrogenation. *Dalton T.* **2014**, 43 (40), 15138–15142.
- (21) Vile, G.; Perez-Ramirez, J. Beyond the use of modifiers in selective alkyne hydrogenation: silver and gold nanocatalysts in flow mode for sustainable alkene production. *Nanoscale* **2014**, 6 (22), 13476–13482.
- (22) Shekhar, M.; Wang, J.; Lee, W.-S.; Williams, W. D.; Kim, S. M.; Stach, E. A.; Miller, J. T.; Delgass, W. N.; Ribeiro, F. H. Size and Support Effects for the Water–Gas Shift Catalysis over Gold Nanoparticles Supported on Model Al<sub>2</sub>O<sub>3</sub> and TiO<sub>2</sub>. *J. Am. Chem. Soc.* **2012**, 134 (10), 4700–4708.
- (23) Bansode, A.; Tidona, B.; von Rohr, P. R.; Urakawa, A. Impact of K and Ba promoters on CO<sub>2</sub> hydrogenation over Cu/Al<sub>2</sub>O<sub>3</sub> catalysts at high pressure. *Catal. Sci. Technol.* **2013**, 3 (3), 767–778.
- (24) Larmier, K.; Liao, W.-C.; Tada, S.; Lam, E.; Verel, R.; Bansode, A.; Urakawa, A.; Comas-Vives, A.; Copéret, C. CO<sub>2</sub>-to-methanol hydrogenation on zirconia-supported copper nanoparticles: reaction intermediates and the role of the metal–support interface. *Angew. Chem., Int. Ed.* **2017**, 56 (9), 2318–2323.
- (25) Wang, J.; Xu, X.; Deng, J.; Liao, Y.; Hong, B. *In situ* Raman spectroscopy studies on the methanol oxidation over silver surface. *Appl. Surf. Sci.* **1997**, 120 (1–2), 99–105.
- (26) Clarke, D. B.; Bell, A. T. An infrared study of methanol synthesis from CO<sub>2</sub> on clean and potassium-promoted Cu/SiO<sub>2</sub>. *J. Catal.* **1995**, 154 (2), 314–328.
- (27) Bando, K. K.; Sayama, K.; Kusama, H.; Okabe, K.; Arakawa, H. *In-situ* FT-IR study on CO<sub>2</sub> hydrogenation over Cu catalysts supported on SiO<sub>2</sub>, Al<sub>2</sub>O<sub>3</sub>, and TiO<sub>2</sub>. *Appl. Catal., A* **1997**, 165 (1), 391–409.
- (28) Fisher, I. A.; Bell, A. T. *In situ* infrared study of methanol synthesis from H<sub>2</sub>/CO<sub>2</sub> over Cu/SiO<sub>2</sub> and Cu/ZrO<sub>2</sub>/SiO<sub>2</sub>. *J. Catal.* **1998**, 178 (1), 153–173.
- (29) Giannozzi, P.; Andreussi, O.; Brumme, T.; Bunau, O.; Buongiorno Nardelli, M.; Calandra, M.; Car, R.; Cavazzoni, C.; Ceresoli, D.; Cococcioni, M.; Colonna, N.; Carnimeo, C.; Dal Corso, A.; de Gironcoli, S.; Delugas, P.; DiStasio, R. A.; Ferretti, A.; Floris, A.; Fratesi, G.; Fugallo, G.; Gebauer, R.; Gerstmann, U.; Giustino, F.; Gorni, T.; Jia, J.; Kawamura, M.; Ko, H.-Y.; Kokalj, A.; Küçükbenli, E.; Lazzeri, M.; Marsili, M.; Marzari, M.; Mauri, F.; Nguyen, N. L.; Nguyen, H.-V.; Otero-de-la-Roza, A.; Paulatto, L.; Poncè, S.; Rocca, D.; Sabatini, R.; Santra, B.; Schlipf, M.; Seitsonen, A. P.; Smogunov, A.; Timrov, I.; Thonhauser, T.; Umari, P.; Vast, N.; Wu, X.; Baroni, S. Advanced Capabilities for Materials Modelling with Quantum ESPRESSO. *J. Phys.: Condens. Matter* **2017**, 29 (46), 465901.
- (30) Perdew, J. P.; Burke, K.; Ernzerhof, M. Generalized gradient approximation made simple. *Phys. Rev. Lett.* **1996**, 77 (18), 3865–3868.
- (31) Grimme, S. Semiempirical GGA-type density functional constructed with a long-range dispersion correction. *J. Comput. Chem.* **2006**, 27 (15), 1787–1799.
- (32) Urakawa, A.; Maeda, N.; Baiker, A. Space- and Time-Resolved Combined DRIFT and Raman Spectroscopy: Monitoring Dynamic Surface and Bulk Processes during NO<sub>x</sub> Storage Reduction. *Angew. Chem., Int. Ed.* **2008**, 47 (48), 9256–9259.
- (33) Ueno, A.; Bennett, C. O. Infrared study of CO<sub>2</sub> adsorption on SiO<sub>2</sub>. *J. Catal.* **1978**, 54 (1), 31–41.
- (34) Roque-Malherbe, R.; Polanco-Estrella, R.; Marquez-Linares, F. Study of the Interaction between Silica Surfaces and the Carbon Dioxide Molecule. *J. Phys. Chem. C* **2010**, 114 (41), 17773–17787.
- (35) McCool, B.; Tripp, C. P. Inaccessible hydroxyl groups on silica are accessible in supercritical CO<sub>2</sub>. *J. Phys. Chem. B* **2005**, 109 (18), 8914–8919.
- (36) Comas-Vives, A. Amorphous SiO<sub>2</sub> surface models: energetics of the dehydroxylation process, strain, ab initio atomistic thermodynamics and IR spectroscopic signatures. *Phys. Chem. Chem. Phys.* **2016**, 18 (10), 7475–7482.
- (37) Bansode, A.; Urakawa, A. Towards full one-pass conversion of carbon dioxide to methanol and methanol-derived products. *J. Catal.* **2014**, 309, 66–70.
- (38) Gaikwad, R.; Bansode, A.; Urakawa, A. High-pressure advantages in stoichiometric hydrogenation of carbon dioxide to methanol. *J. Catal.* **2016**, 343, 127–132.
- (39) Lam, E.; Larmier, K.; Wolf, P.; Tada, S.; Safonova, O. V.; Copéret, C. Isolated Zr Surface Sites on Silica Promote Hydrogenation of CO<sub>2</sub> to CH<sub>3</sub>OH in Supported Cu Catalysts. *J. Am. Chem. Soc.* **2018**, 140 (33), 10530–10535.